

# Geophysical Research Letters<sup>®</sup>

## RESEARCH LETTER

10.1029/2024GL112848

Yifeng Cheng and Lu Wang contributed equally to this work.

### Key Points:

- Spring sea surface temperature over the tropical West Pacific is used as an observational constraint for future monsoon onset projections
- Autumn surface warming trends over northern mid-high latitudes can constrain future changes in monsoon withdrawal
- Constrained projections show a more reliable reduction in Indian summer monsoon duration compared to unconstrained projections

### Supporting Information:

Supporting Information may be found in the online version of this article.

### Correspondence to:

L. Wang,  
luwang@nuist.edu.cn

### Citation:

Cheng, Y., Wang, L., Chen, X., Zhou, T., & Turner, A. (2025). A shorter duration of the Indian summer monsoon in constrained projections. *Geophysical Research Letters*, 52, e2024GL112848. <https://doi.org/10.1029/2024GL112848>

Received 30 SEP 2024  
Accepted 20 DEC 2024

## A Shorter Duration of the Indian Summer Monsoon in Constrained Projections



Yifeng Cheng<sup>1</sup>, Lu Wang<sup>1,2</sup> , Xiaolong Chen<sup>3</sup> , Tianjun Zhou<sup>3,4</sup> , and Andrew Turner<sup>5,6</sup>

<sup>1</sup>Key Laboratory of Meteorological Disaster, Ministry of Education (KLME) / Collaborative Innovation Center on Forecast and Evaluation of Meteorological Disasters (CIC-FEMD), Nanjing University of Information Science and Technology, Nanjing, China, <sup>2</sup>Laboratory for Regional Oceanography and Numerical Modeling, Qingdao Marine Science and Technology Center, Qingdao, China, <sup>3</sup>State Key Laboratory of Numerical Modeling for Atmospheric Sciences and Geophysical Fluid Dynamics, Institute of Atmospheric Physics, Chinese Academy of Sciences, Beijing, China, <sup>4</sup>College of Earth and Planetary Sciences, The University of Chinese Academy of Sciences, Beijing, China, <sup>5</sup>National Centre for Atmospheric Science, University of Reading, Reading, UK, <sup>6</sup>Department of Meteorology, University of Reading, Reading, UK

**Abstract** A reliable projection of the future duration of the Indian summer monsoon (ISM) provides an important input for climate adaptation in the Indian subcontinent. Nevertheless, there is low confidence for projections of ISM duration, due to large inter-model uncertainty of onset and withdrawal changes. Here, we find that models with excessive sea surface temperature (SST) over the tropical western Pacific (WP) during spring and greater surface warming trends over the northern mid-high latitudes (NMHL) during autumn in the present day tend to overestimate future delays to ISM onset and withdrawal, respectively. This can be attributed to the influence of surface thermal conditions on upper-tropospheric warming patterns. Constrained by the observational WP SST and NMHL surface warming trends, projected ISM duration under a high-emission scenario is shortened by 6 days compared to the current climate, with a reduction of inter-model uncertainty by 46% relative to the unconstrained results.

**Plain Language Summary** The duration of the Indian summer monsoon (ISM) has profound implications for socioeconomic activity in the Indian subcontinent, given its strong link with the length of India's rainy season, which directly impacts water resources, crops and fisheries. The potential future change of ISM duration remains inconclusive due to large inter-model discrepancies between models. Here, we find that the model uncertainties of climatic change in the onset and withdrawal of the ISM are closely related to the modeled present-day sea surface temperatures in the tropical western Pacific Ocean and the surface warming trend over Northern Hemisphere mid-high latitudes, respectively. By constraining present-day simulations of the two metrics using observations, the projected ISM duration becomes shorter, and the uncertainty is reduced significantly in comparison to unconstrained estimates. The results imply that more and more intense extreme rainfall events will occur within a shorter season, which will significantly increase the impact of the hydrological disasters associated with extreme rainfall events such as flash floods and landslides.

## 1. Introduction

The Indian summer monsoon (ISM) is one of the world's most energetic monsoon systems, featuring a sudden onset in late May/early June and a gradual withdrawal in late September/early October (Ananthakrishnan & Soman, 1988; Goswami et al., 1999; Webster & Yang, 1992). The duration of the ISM has profound implications for the socioeconomic activity of people living in the Indian subcontinent, who account for over 20% of the global population. A shortened ISM duration amounts to a shorter rainy season over India (Goswami & Xavier, 2005), resulting in a dry ISM (Misra et al., 2017), which reduces cultivated area and crop yields (Bandurathna et al., 2021; Subash et al., 2023). Conversely, a longer ISM duration extends the fishing moratorium period in South Asia (Islam et al., 2021). Thus, a reliable prediction of ISM duration is crucial for effective agricultural planning, water-resource management and fisheries in this densely populated region.

The future global warming that is inevitable due to anthropogenic greenhouse gas forcing will undoubtedly impact the characteristics of the ISM, such as causing an increasing trend in ISM precipitation (Luo et al., 2024; Rajesh et al., 2021; Saha et al., 2023; Turner & Annamalai, 2012). However, there is still a lack of reliable projections regarding how the duration of the ISM will change in the future (Wang et al., 2024). This is due to the large discrepancy in the projected ISM duration changes between models (Dong et al., 2016; Ha et al., 2020;

© 2025. The Author(s).

This is an open access article under the terms of the Creative Commons Attribution License, which permits use, distribution and reproduction in any medium, provided the original work is properly cited.

Kitoh et al., 2013; Lv et al., 2024; Moon & Ha, 2017; Zhang et al., 2012; Zhou et al., 2024). According to the latest Coupled Model Intercomparison Project (CMIP) multi-model results (i.e., CMIP6), there is “low confidence” in projections of ISM duration (Ha et al., 2020). This uncertainty in ISM duration projections is hindering efforts to plan and adapt to changes in risk. Hence a reliable projection of the ISM duration is of crucial importance to climate adaptation activities.

The emergent constraint technique is one of the most promising methods to reduce uncertainties in future projections; it is based on physical understanding and the exploitation of statistical relationships between observable quantities from present-day simulations in future climate projections (Chen et al., 2020; Deangelis et al., 2015; Donat et al., 2018; Hall & Qu, 2006; He, 2023; Li & Xie, 2014; Li et al., 2023). This technique has been previously applied to constrain projections of Indian summer precipitation (Chen et al., 2022; Li et al., 2016, 2017; Rajesh & Goswami, 2022; Shamal & Sanjay, 2021). In this study, we aim to reveal the potential sources of uncertainty in the projection of ISM duration, and explore the possibility of adopting emergent constraints for future ISM duration changes using multiple CMIP6 model simulations. Our results suggest a shorter ISM duration in a future warming climate than the unconstrained estimates.

## 2. Materials and Methods

The outputs of historical simulations and future projections under the very-high-greenhouse-gas emission scenario (SSP5-8.5) from 24 CMIP6 models (Table S1 in Supporting Information S1) are used in our analysis, and the first available member (i.e., r1i1p1f1) is used for each model and each experiment in which adequate variables are outputted. The models were selected based on the availability of daily air temperature, as it is a prerequisite for defining the ISM duration in this study.

In addition, multiple observational data sets of sea surface temperature (SST) and surface temperature (Ts) are utilized. The SST data sets were derived from six sources: COBE-SST (Ishii et al., 2005), COBE-SST2 (Hirahara et al., 2014), ERSSTv3 (Smith et al., 2008), ERSSTv5 (Huang et al., 2017), HadISST (Rayner et al., 2003), and ICOADS (Freeman et al., 2017), while the Ts data sets were derived from four sources: BEST (Rohde et al., 2013), Cowtan and Way version 2 (Cowtan et al., 2014), GISTEMP v5 (Lenssen et al., 2019), and NOAAGlobalTemp v5 (Vose et al., 2012). All model outputs and observations are remapped onto a uniform resolution 2.5°-grid using bilinear interpolation. The historical climatology is calculated from 1960 to 2010, while the future climatology is calculated from 2049 to 2099. Their difference (future minus history) is calculated as the projected change.

The ISM duration is determined by the onset and withdrawal dates of the ISM. Following previous studies (Goswami & Xavier, 2005; Liu & Yanai, 2001; Sabeerali & Ajayamohan, 2018; Wu & Liu, 2014; Xavier et al., 2007), the ISM onset and withdrawal dates can be estimated by the reversal of the meridional gradient of upper tropospheric (500–250 hPa) temperature (UTT) over India. In this study, the ISM onset (withdrawal) date is defined as the day on which the daily climatology of the meridional gradient of UTT, averaged over the Indian subcontinent (10°–30°N, 70°–85°E; marked in Figure S1a in Supporting Information S1), undergoes a reversal from negative to positive (positive to negative). Based on this definition, the observational ISM onsets in early June and withdraws in late September (red curve in Figure S1b in Supporting Information S1). This feature can be captured by the multi-model mean results from CMIP6 models very well (black curve in Figure S1b in Supporting Information S1), albeit with some inter-model discrepancies (gray curves in Figure S1b in Supporting Information S1). The onset and withdrawal dates derived from the current definition are not sensitive to the specific regions used for the meridional gradient of UTT (Figure S2 in Supporting Information S1).

The hierarchical emergent constraint framework proposed by Bowman et al. (2018) is used to constrain the projection of the ISM duration (see Supplementary Text S1 in Supporting Information S1).

## 3. Results

### 3.1. Projection Uncertainty in the ISM Duration Across Models

Figure 1a presents the future changes in the ISM onset and withdrawal dates from each model. These projections reveal a notable variability among models, with standard deviations of 4.1 days for the onset and 3.6 days for the withdrawal (marked by the red bars). These inter-model discrepancies even surpass the multi-model mean changes (marked by the large red dot). The considerable uncertainty in projections of the onset and withdrawal

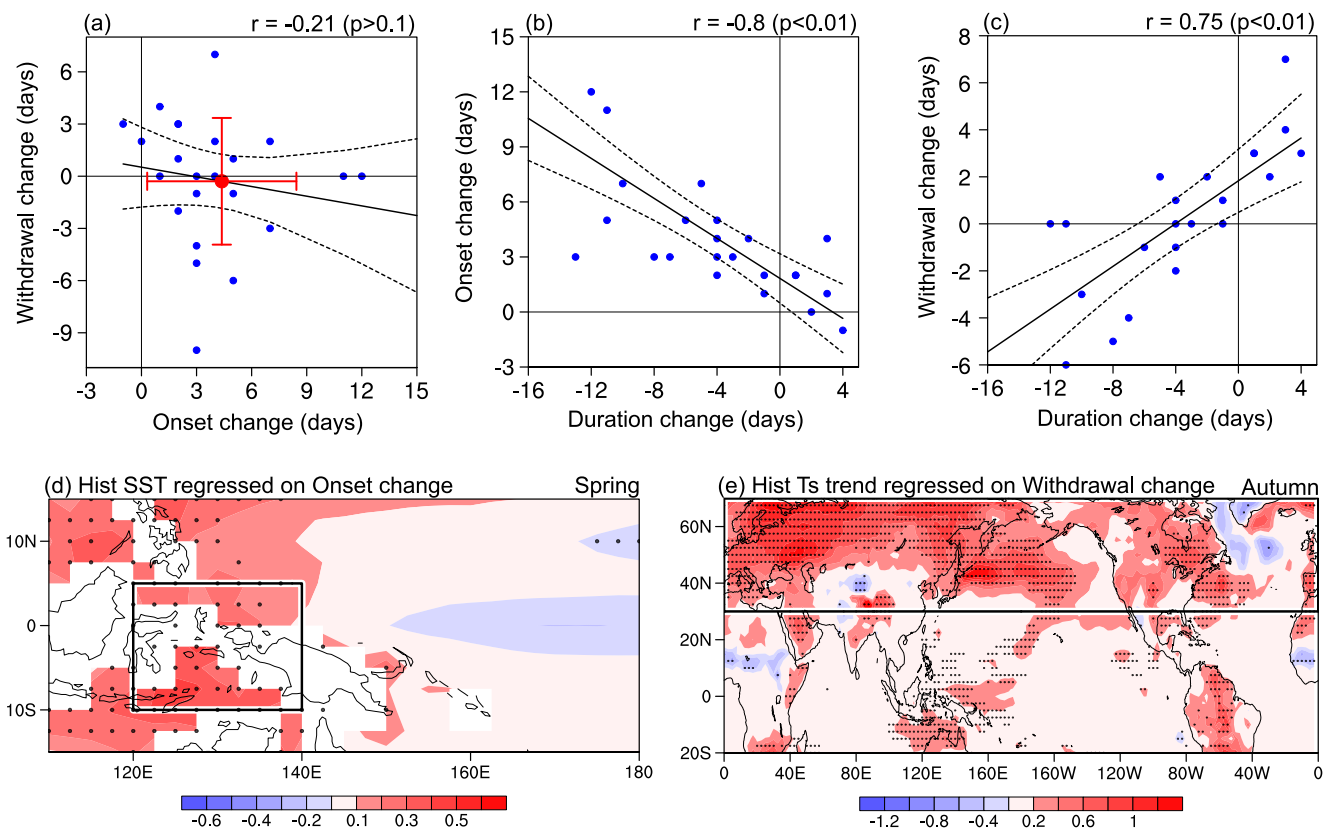


**Figure 1.** Inter-model relationship between future temporal shift (units: days) of the ISM: (a) onset versus withdrawal, (b) duration versus onset, and (c) duration versus withdrawal. Solid best-fit line is obtained using the least squares method, and dashed curves denote the 95% confidence range of this linear fit. The inter-model correlation coefficient ( $r$ ) and p-value are shown on the top-right corner. The red dot (line) in (a) denotes the multi-model mean (one inter-model standard deviation). Spatial pattern of (d) historical SST ( $^{\circ}$ C) in the spring (February-April) mean corresponding to future changes in ISM onset and (e) historical surface temperature trend ( $^{\circ}$ C yr $^{-1}$ ) from 1960 to 2010 during autumn (September-October) corresponding to withdrawal changes, obtained by regression against the normalized future onset and withdrawal changes, respectively. The tropical mean SST between 15°S and 15°N in the present was removed from each model before regression. The stippling in (d), (e) represents a regression statistically significant at the 90% confidence level according to the Student's  $t$ -test. The black rectangle in (d) marks the 10°S–5°N, 120°E–140°E domain (WP) and in (e) denotes the 30°N–70°N, 0°–360°E domain (NMHL).

can lead to a high uncertainty in the projected changes of the ISM duration. This is also supported by the high inter-model correlation between the projected changes in the ISM duration and those in the onset ( $r = -0.8$ ,  $p < 0.01$ ; Figure 1b) and withdrawal dates ( $r = 0.75$ ,  $p < 0.01$ ; Figure 1c).

It is noteworthy that the projected changes in the onset and withdrawal dates exhibit very low correlation relationship ( $r = -0.21$ ,  $p > 0.1$ ; Figure 1a). This suggests that the sources for the inter-model discrepancies in the projections of onset and withdrawal dates should be different, which thus need to be investigated separately.

### 3.2. Emergent Relationship Between Historical Simulations and Projections of ISM Duration

The ISM duration is closely related to the reversal of the thermal contrast between the tropics and the northern subtropics during the transition seasons. To understand the uncertainty in ISM onset and withdrawal projections, we focus on the thermal conditions in spring and autumn, as they are critical in the transition of the monsoon circulation. The association between the current SST/surface temperature trend during the transition seasons and the future changes in the ISM onset/withdrawal dates were examined respectively to identify the emergent relationships. A significant positive correlation is found between future changes in the ISM onset and the current SST over the tropical West Pacific (WP) in the spring (February-April) mean (Figure 1d), indicating that a model with a warmer WP SST during spring in the present-day climate will project a more delayed onset of the ISM in future. Regarding the ISM withdrawal projections, a significant positive correlation pattern was obtained between these and the current 1960–2010 surface temperature trend over the northern mid-high latitudes (NMHL) during

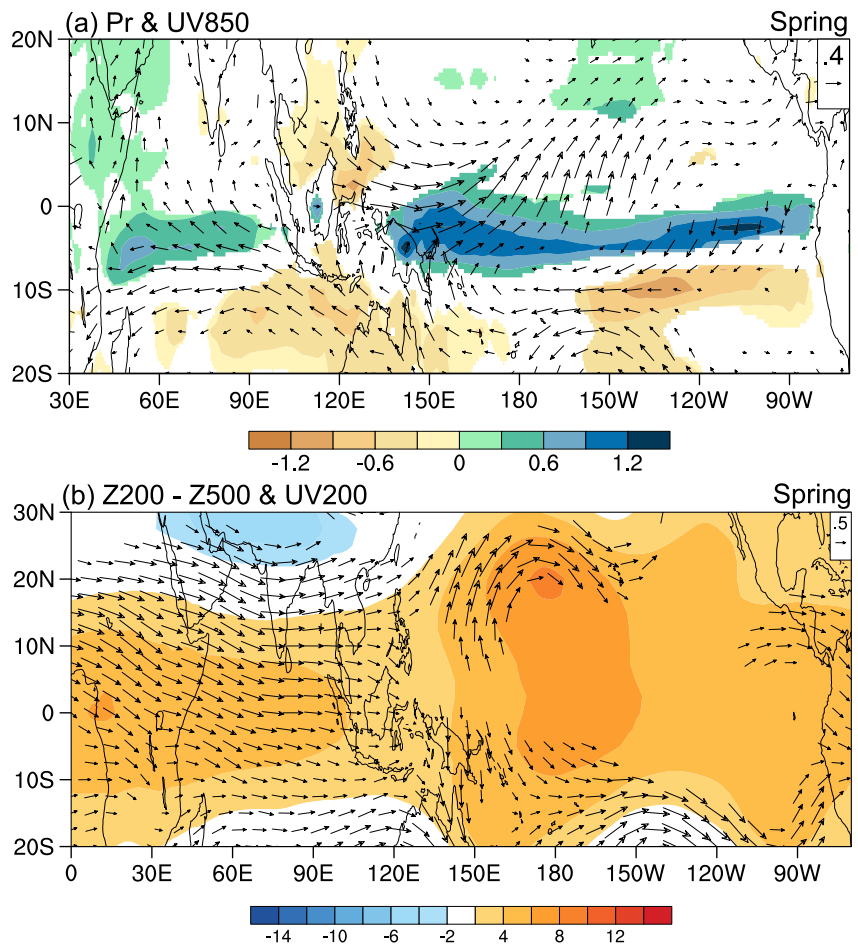


**Figure 2.** Spatial pattern of future changes in spring (a) precipitation (shading shown above the 90% significance level;  $\text{mm day}^{-1}$ ) and 850-hPa wind (vector;  $\text{m s}^{-1}$ ), and (b) 500–200 hPa thickness (shading; m) and 200-hPa wind (vectors;  $\text{m s}^{-1}$ ) regressed onto the normalized present-day  $SST_{WP}$ .

autumn (September–October) (Figure 1e). This pattern indicates that models exhibiting a stronger surface warming in the NMHL in the historical period tend to project a more delayed ISM withdrawal in future.

Why does a significant inter-model correlation between the present-day WP SST and temporal shift in the future ISM onset exist? To understand this, we define an SST index as the average of current SST over the  $10^{\circ}\text{S}$ – $5^{\circ}\text{N}$ ,  $120^{\circ}\text{E}$ – $140^{\circ}\text{E}$  domain (marked by the rectangle in Figure 1d) relative to the tropical mean ( $15^{\circ}\text{S}$ – $15^{\circ}\text{N}$ ,  $0^{\circ}$ – $360^{\circ}\text{E}$ ) in spring (February–April) (hereafter  $SST_{WP}$ ), and then regress the projected precipitation and circulation changes onto the normalized  $SST_{WP}$  (Figure 2). The results show that models with a warmer WP SST in the present will project a greater increase in precipitation over the equatorial western-central Pacific in the future (Figure 2a). This intensified precipitation anomaly then leads to changes in tropical circulation as predicted by the Gill model (Gill, 1980), including a pair of off-equatorial cyclonic gyres to its west and equatorial easterly winds to its east in the lower levels, with a reverse pattern in the upper troposphere. Moreover, it can trigger upper tropospheric warming through condensational latent heat release. Subsequently, this warm anomaly rapidly propagates across the tropics through the equatorial wave adjustment process (Neelin & Su, 2005; Su et al., 2003; Xie et al., 2010) and thus lead to warmer UTT over the entire tropics (Figure 2b). This warming pattern in the upper troposphere contributes to delaying the ISM onset by hindering the reversal of the meridional gradient of UTT from negative to positive.

Recent studies (Cheng et al., 2024; Pathirana et al., 2024) have provided a physical explanation for the connection between present-day WP SST and future precipitation changes over the equatorial western-central Pacific. In these studies, the future precipitation changes over the western-central Pacific are closely related to the

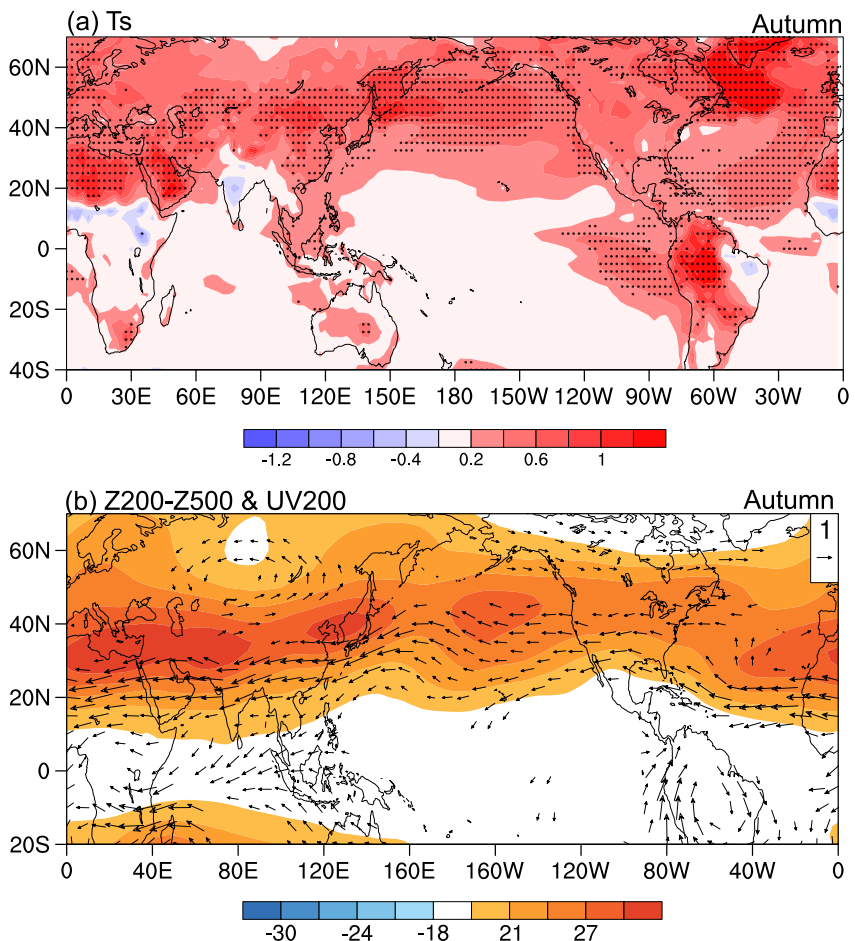


**Figure 3.** Spatial pattern of future changes in autumn (a) surface temperature ( $^{\circ}\text{C}$ ), and (b) 500–200 hPa thickness (shading; m) and 200-hPa wind (vectors;  $\text{m s}^{-1}$ ), regressed onto the normalized  $\text{TsTr}$ , representing the present-day surface warming trend over the NMHL. Black dots in (a) indicate the 90% significance level.

precipitation sensitivity over this region, as evidenced by their significant positive correlation ( $r = 0.47, p < 0.05$ ; Figure S3a in Supporting Information S1). Here, the precipitation sensitivity is defined as the linear response of precipitation to the SST over the region ( $10^{\circ}\text{S}$ – $10^{\circ}\text{N}$ ,  $120^{\circ}$ – $170^{\circ}\text{E}$ ) on an interannual time scale. The positive correlation suggests that models with higher precipitation sensitivity will project a greater precipitation increase for the same SST rise in the future. Furthermore, the precipitation sensitivity of the western-central Pacific is influenced by the current WP SST in spring, as they are significantly correlated ( $r = 0.54, p < 0.01$ , Figure S3b in Supporting Information S1).

How does the NMHL surface warming trend in recent decades affect projected changes in the ISM withdrawal? Here, following Chen et al. (2022), we define a surface temperature trend index to represent the present-day NMHL warming pattern (hereafter  $\text{TsTr}$ ). For the  $\text{TsTr}$  of each model, the historical surface warming trend from 1960 to 2010 in autumn (September–October) in each model is projected onto the inter-model warming trend shown in Figure 1e over the  $30^{\circ}\text{N}$ – $70^{\circ}\text{N}$ ,  $0^{\circ}$ – $360^{\circ}\text{E}$  domain (marked by the rectangle in Figure 1e). Then, we regress the projected surface temperature and circulation changes onto  $\text{TsTr}$  (Figure 3). A significant surface warming pattern is obtained over the NMHL, indicating that a model with a larger NMHL warming trend will project a greater increase in surface temperature over the same region (Figure 3a). Additionally, a warmer upper troposphere over the northern middle latitudes is also seen, as indicated by the increase of atmospheric layer thickness (Figure 3b). The warming patterns of the upper troposphere and the surface temperature are generally consistent, indicating that the atmospheric temperature change is probably influenced by the surface temperature change, as a warmer surface could release more upward sensible heat flux and thereby warm the atmospheric column (Cohen et al., 2019; Myhre et al., 2018). The upper-tropospheric thermal contrast between the northern

midlatitudes and tropics favors postponement of the ISM withdrawal, as it hinders reversal of the meridional gradient of UTT from positive to negative.

A greater warming in the NMHL than the rest of the globe is inherent to global warming, due to the smaller heat capacity from a larger land area fraction in this region (Byrne & O’Gorman, 2013; Previdi et al., 2021). Hence, the inter-model spread in the global mean warming rate under a given radiative forcing can influence the inter-model spread in the NMHL warming trend in recent decades, as well as that in the future surface temperature change of the NMHL (Chen et al., 2022; Tokarska et al., 2020). As shown in Figures S4a and S4b in Supporting Information S1, the equilibrium climate sensitivity, which measures the global mean warming rate, is significantly correlated with the TsTr ( $r = 0.58, p < 0.01$ ), and the surface temperature change averaged over  $30^{\circ}\text{N}$ – $70^{\circ}\text{N}, 0$ – $360^{\circ}\text{E}$  ( $r = 0.82, p < 0.01$ ). Thus, models showing a stronger warming trend over the NMHL would induce a greater increase in surface temperature in the future and thereby warmer air temperature in that region, finally resulting in greater postponement in the reversal of the meridional gradient of UTT from positive to negative, that is a delayed ISM withdrawal.

The underlying mechanisms provide a solid physical basis for the observational constraint. Thus, we can constrain the future inter-model uncertainty of ISM onset and withdrawal based on the current observed SST over the WP in spring and observed surface warming trend over the NMHL in autumn, respectively.

### 3.3. Constrained Projection of ISM Duration

To constrain the inter-model uncertainty in projecting the ISM duration, we first constrain the uncertainty in onset and withdrawal changes, respectively. For the ISM onset, the  $SST_{\text{WP}}$  defined in Section 3.2 is used as the observational constraint. The inter-model variations of  $SST_{\text{WP}}$  and the projected ISM onset show a significant correlation of 0.57 (Figure 4a), indicating that the inter-model spread in simulating the current WP SST can explain around 32% of the inter-model spread in ISM onset projections. The model results are further compared with the observational  $SST_{\text{WP}}$  based on six observational data sets (vertical purple shading in Figure 4a). The climatological values of  $SST_{\text{WP}}$  in  $\sim 70\%$  models are larger than those in observations, indicating a systematic overestimation of the current WP SST by CMIP6 models. The constrained projections show that the ISM onset will be delayed by 3 days in the future, which is one day less than the original projection that showed a 4-day delay in the ISM onset (Figure 4c). Furthermore, the probability density function of constrained ISM onset projection is narrower than the unconstrained one, with a reduction in inter-model variance of 39%.

Regarding the ISM withdrawal, the TsTr defined in Section 3.2 is used as the observational constraint. The inter-model variations of TsTr and the projected ISM withdrawal dates show a significant correlation of 0.76 (Figure 4b), indicating that the inter-model spread in simulating the current NMHL surface warming can explain around 58% of the inter-model spread in the ISM withdrawal projections. The model results are further compared with the observational TsTr based on four observational data sets (vertical purple shading in Figure 4b), which shows that most models overestimate the current warming trend, consistent with previous studies (Chen et al., 2022; Tokarska et al., 2020). The constrained projections show that the ISM withdrawal will advance by 3 days in the future, in contrast to the unconstrained projections showing minimal change (Figure 4d). Additionally, the inter-model variance of the projected ISM withdrawal is reduced by 56% after the observational constraint.

The constrained projection of ISM duration, based on constrained projections of the ISM onset and withdrawal, shows a 46% reduction in the inter-model variance compared to the raw projection (Figure 4e). Additionally, it suggests that the ISM duration will be shortened by 6 days in the future. By contrast, the unconstrained projection of the ISM duration is not reliable due to a much higher inter-model uncertainty.

## 4. Conclusions

A reliable projection of the Indian summer monsoon duration is critical for effective planning for agriculture, water resources and fisheries over the Indian subcontinent. However, existing projections show large inter-model uncertainties, jointly contributed by model discrepancies in projecting changes in the ISM onset and withdrawal. We found that models with higher SST over the tropical WP during spring in the present tend to overestimate the future delay of ISM onset. The relationship is attributed to different precipitation sensitivities across models. Models with warmer WP SST tend to project a greater increase in precipitation over the western-central Pacific in

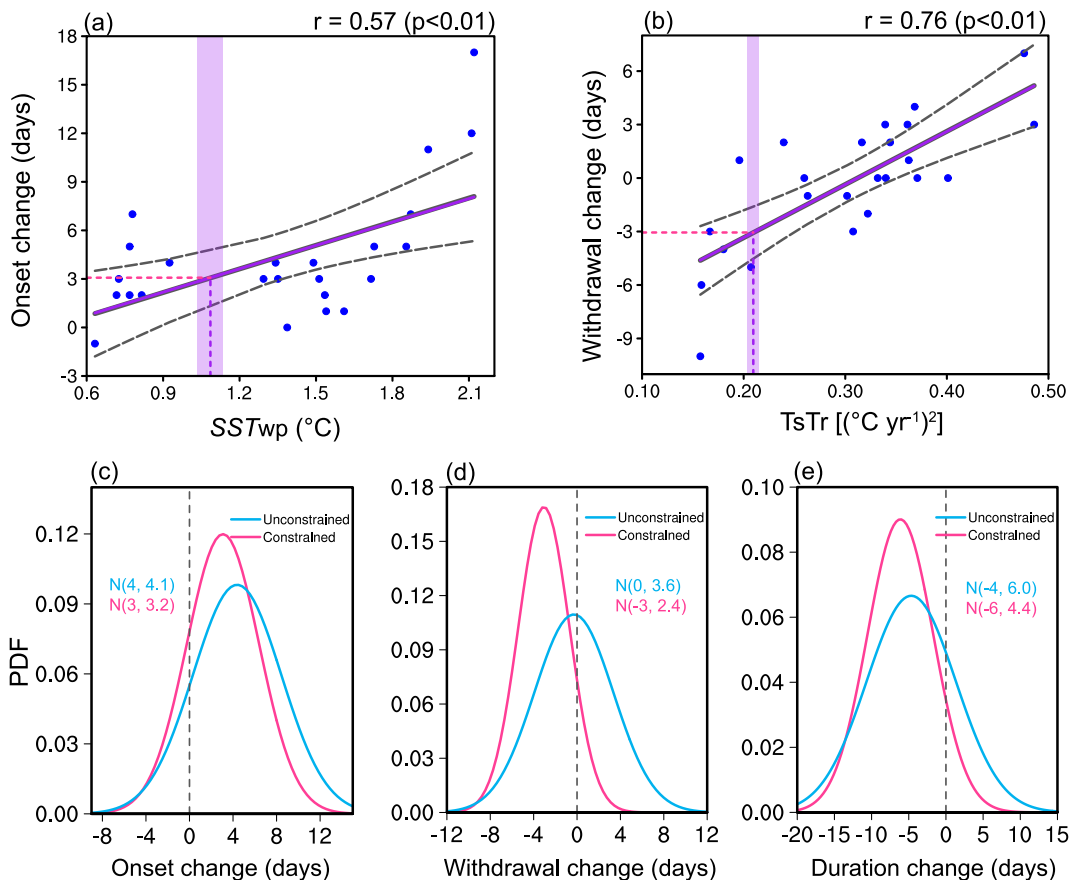


**Figure 4.** (Upper panels) Inter-model relationship between current measurements and future temporal shifts of the ISM: (a)  $SST_{WP}$  (°C) versus onset change (days), (b)  $TsTr$  [ $(^{\circ}\text{C yr}^{-1})^2$ ] versus withdrawal change (days). The inter-model correlation coefficient ( $r$ ) and p-value are shown on the top-right corner. The gray best-fit line is obtained using the least squares method, and dashed curves denote the 95% confidence range of the fit. The observations are denoted by vertical purple color, with the line (shading) representing the mean (one standard deviation) of different observational data sets. The purple best-fit line is obtained by correcting the gray best-fit line using observations. The horizontal violet-red line represents the constrained projection result (Lower panels) Probability density function (PDF) under a Gaussian assumption of the unconstrained and constrained future projections in the (c) onset, (d) withdrawal, and (e) duration of the ISM. The values in parentheses are mean and standard deviation of the Gaussian distribution.

the future, thereby leading to a higher rise in UTT due to condensational latent heat release, which could propagate throughout the tropics via equatorial wave adjustment process. The greater warming in the tropics than in the northern latitudes hinders the reversal of the meridional gradient of UTT from negative to positive, thus contributing to a delay in the ISM onset. The projected ISM withdrawal is affected by the NMHL warming, as models with a greater surface warming trend over the NMHL during autumn in the present tend to overestimate the future withdrawal. This relationship is attributed to the diverse response of the surface temperature change to a given radiative forcing across models. Models showing a stronger historical NMHL warming trend would induce a greater increase in future surface temperature over this region, thereby warming the UTT through sensible heat fluxes. The greater warming of the NMHL than the tropics in the upper troposphere hinders the reversal of the meridional gradient of UTT from positive to negative and thus contributes to the delay of the ISM withdrawal.

We further use the WP SST in spring and the NMHL surface temperature trend in autumn as observational constraints to correct the projections of ISM onset and withdrawal respectively. The constrained projections show that the ISM duration—using a metric based on tropospheric temperature—will be shortened by ~6 days in the future, due to ~3 days delay in onset and ~3 days advance in withdrawal. The inter-model variance of the ISM duration projections has been reduced by 46% in the constrained results compared to the raw projection, with a 39% reduction in the onset and a 56% reduction in the withdrawal.

The results suggest that the Indian rainy season is likely to be shortened. More importantly, although the shrinking of the Indian rainy season tends to restrict the increasing trend of ISM accumulated rainfall in the future, ISM accumulated rainfall and the frequency and intensity of daily extreme rainfall events are expected to increase under global warming (Rajesh et al., 2021). This suggests that more and more intense extreme rainfall events will occur within a shorter season, which will significantly increase the impact of the hydrological disasters associated with extreme rainfall events such as flash floods and landslides.

As the future shrinking of the ISM duration is analogous to that observed in El Niño years, and the El Niño can also influence the ISM duration through its effect on UTT (Goswami & Xavier, 2005; Sabeer Ali et al., 2012; Sahana et al., 2015; Xavier et al., 2007), it seems reasonable to suggest that the changing nature of El Niño under global warming (Chen et al., 2015, 2017) may be an important factor in reducing the length of ISM in the future. However, given that La Niña years tend to lengthen the ISM, the net effect on the ISM duration averaged over many events would be zero. It is acknowledged that ENSO itself is skewed (Chen et al., 2016, 2019; Sun et al., 2023), and therefore the impacts on the ISM duration may not be linear, and may not cancel each other out. This indicates the necessity for further research to ascertain the precise role of ENSO in the projected change of ISM duration.

## Data Availability Statement

The CMIP6 models used in this study are listed in Table S1 in Supporting Information S1, available from the Earth System Grid Federation at <https://esgf-node.llnl.gov/search/cmip6/>. Observational SST data HadISST are downloaded at <https://www.metoffice.gov.uk/hadobs/>, ERSSTv3, ERSSTv5, ICOADS, COBE-SST, and COBE-SST2 are downloaded at <https://www.esrl.noaa.gov/psd/data/gridded/tables/sst.html>. Observational Ts data BEST are available at <http://berkeleyearth.org/data-new/>, Cowtan and Way v2 are available at <https://www-users.york.ac.uk/~kdc3/papers/coverage2013/series.html>, GISTEMP v5 are available at <https://data.giss.nasa.gov/gistemp/>, NOAA GlobalTemp v5 are available at <https://psl.noaa.gov/data/gridded/>.

## Acknowledgments

The work is supported by the National Key Research and Development Program of China (Grant 2020YFA0608901). AT was funded by the MiLCMOP project (Natural Environment Research Council Grant NE/X000176/1). We acknowledge the High Performance Computing Center of Nanjing University of Information Science & Technology for their support of this work.

## References

- Ananthakrishnan, R., & Soman, M. K. (1988). The onset of the southwest monsoon over Kerala: 1901–1980. *Journal of Climatology*, 8(3), 283–296. <https://doi.org/10.1002/joc.3370080305>
- Bandurathna, L. A. D. B., Wang, L., Zhou, X., Cheng, Y., & Chen, L. (2021). Intraseasonal oscillation of the southwest monsoon over Sri Lanka and evaluation of its subseasonal forecast skill. *Atmospheric and Oceanic Science Letters*, 14(6), 100062. <https://doi.org/10.1016/j.asol.2021.100062>
- Bowman, K. W., Cressie, N., Qu, X., & Hall, A. (2018). A hierarchical statistical framework for emergent constraints: Application to snow-albedo feedback. *Geophysical Research Letters*, 45(23), 13050–13059. <https://doi.org/10.1029/2018gl080082>
- Byrne, M. P., & O’Gorman, P. A. (2013). Land–ocean warming contrast over a wide range of climates: Convective quasi-equilibrium theory and idealized simulations. *Journal of Climate*, 26(12), 4000–4016. <https://doi.org/10.1175/JCLI-D-12-0026.1>
- Chen, L., Li, T., Behera, S. K., & Doi, T. (2016). Distinctive precursory air-sea signals between regular and super El Niños. *Advances in Atmospheric Sciences*, 33(8), 996–1004. <https://doi.org/10.1007/s00376-016-5250-8>
- Chen, L., Li, T., & Yu, Y. (2015). Causes of strengthening and weakening of ENSO amplitude under global warming in four CMIP5 models. *Journal of Climate*, 28(8), 3250–3274. <https://doi.org/10.1175/JCLI-D-14-00439.1>
- Chen, L., Li, T., Yu, Y., & Behera, S. K. (2017). A possible explanation for the divergent projection of ENSO amplitude change under global warming. *Climate Dynamics*, 49(11–12), 3799–3811. <https://doi.org/10.1007/s00382-017-3544-x>
- Chen, L., Sun, D. Z., Wang, L., & Li, T. (2019). A further study on the simulation of cloud-radiative feedbacks in the ENSO cycle in the tropical Pacific with a focus on the asymmetry. *Asia-Pacific Journal of Atmospheric Sciences*, 55(3), 303–316. <https://doi.org/10.1007/s13143-018-0064-5>
- Chen, X., Zhou, T., Wu, P., Guo, Z., & Wang, M. (2020). Emergent constraints on future projections of the western North Pacific subtropical high. *Nature Communications*, 11(1), 2802. <https://doi.org/10.1038/s41467-020-16631-9>
- Chen, Z., Zhou, T., Chen, X., Zhang, W., Zhang, L., Wu, M., & Zou, L. (2022). Observationally constrained projection of Afro-Asian monsoon precipitation. *Nature Communications*, 13(1), 1–12. <https://doi.org/10.1038/s41467-022-30106-z>
- Cheng, Y., Wang, L., Chen, X., Zhou, T., Turner, A., & Wang, L. (2024). Constrained projections indicate less delay in onset of summer monsoon over the Bay of Bengal and South China Sea. *Geophysical Research Letters*, 51(21), e2024GL110994. <https://doi.org/10.1029/2024GL110994>
- Cohen, J., Zhang, X., Francis, J., Jung, T., Kwok, R., Overland, J., et al. (2020). Divergent consensuses on Arctic amplification influence on midlatitude severe winter weather. *Nature Climate Change*, 10(1), 20–29. <https://doi.org/10.1038/s41558-019-0662-y>
- Cowtan, K., & Way, R. G. (2014). Coverage bias in the HadCRUT4 temperature series and its impact on recent temperature trends. *Quarterly Journal of the Royal Meteorological Society*, 140(683), 1935–1944. <https://doi.org/10.1002/qj.2297>
- DeAngelis, A. M., Qu, X., Zelinka, M. D., & Hall, A. (2015). An observational radiative constraint on hydrologic cycle intensification. *Nature*, 528(7581), 249–253. <https://doi.org/10.1038/nature15770>
- Donat, M. G., Pitman, A. J., & Angélil, O. (2018). Understanding and reducing future uncertainty in midlatitude daily heat extremes via land surface feedback constraints. *Geophysical Research Letters*, 45(19), 10–627. <https://doi.org/10.1029/2018GL079128>
- Dong, G., Zhang, H., Moise, A., Hanson, L., Liang, P., & Ye, H. (2016). CMIP5 model-simulated onset, duration and intensity of the Asian summer monsoon in current and future climate. *Climate Dynamics*, 46(1–2), 355–382. <https://doi.org/10.1007/s00382-015-2588-z>

- Freeman, E., Woodruff, S. D., Worley, S. J., Lubker, S. J., Kent, E. C., Angel, W. E., et al. (2017). ICOADS release 3.0: A major update to the historical marine climate record. *International Journal of Climatology*, 37(5), 2211–2232. <https://doi.org/10.1002/joc.4775>
- Gill, A. E. (1980). Some simple solutions for heat-induced tropical circulation. *Quarterly Journal of the Royal Meteorological Society*, 106(449), 447–462. <https://doi.org/10.1002/qj.49710644905>
- Goswami, B. N., Krishnamurthy, V., & Annamalai, H. (1999). A broad-scale circulation index for the interannual variability of the Indian summer monsoon. *Quarterly Journal of the Royal Meteorological Society*, 125(554), 611–633. <https://doi.org/10.1002/qj.49712555412>
- Goswami, B. N., & Xavier, P. K. (2005). ENSO control on the South Asian monsoon through the length of the rainy season. *Geophysical Research Letters*, 32(8), L18717. <https://doi.org/10.1029/2005GL023216>
- Ha, K.-J., Moon, S., Timmermann, A., & Kim, D. (2020). Future changes of summer monsoon characteristics and evaporative demand over Asia in CMIP6 simulations. *Geophysical Research Letters*, 47(8), e2020GL087492. <https://doi.org/10.1029/2020GL087492>
- Hall, A., & Qu, X. (2006). Using the current seasonal cycle to constrain snow albedo feedback in future climate change. *Geophysical Research Letters*, 33(3). <https://doi.org/10.1029/2005GL025127>
- He, C. (2023). Future drying subtropical East Asia in winter: Mechanism and observational constraint. *Journal of Climate*, 36(9), 2985–2998. <https://doi.org/10.1175/JCLI-D-22-0347.1>
- Hirahara, S., Ishii, M., & Fukuda, Y. (2014). Centennial-scale sea surface temperature analysis and its uncertainty. *Journal of Climate*, 27(1), 57–75. <https://doi.org/10.1175/JCLI-D-12-00837.1>
- Huang, B., Thorne, P. W., Banzon, V. F., Boyer, T., Chepurin, G., Lawrimore, J. H., et al. (2017). Extended reconstructed sea surface temperature, version 5 (ERSSTv5): Upgrades, validations, and intercomparisons. *Journal of Climate*, 30(20), 8179–8205. <https://doi.org/10.1175/JCLI-D-16-0836.1>
- Ishii, M., Shouji, A., Sugimoto, S., & Matsumoto, T. (2005). Objective analyses of sea-surface temperature and marine meteorological variables for the 20th century using ICOADS and the Kobe Collection. *International Journal of Climatology*, 25(7), 865–879. <https://doi.org/10.1002/joc.1169>
- Islam, M. M., Begum, A., Rahman, S. M. A., & Ullah, H. (2021). Seasonal fishery closure in the northern Bay of Bengal causes immediate but contrasting ecological and socioeconomic impacts. *Frontiers in Marine Science*, 8, 704056. <https://doi.org/10.3389/fmars.2021.704056>
- Kitoh, A., Endo, H., Kumar, K. K., Cavalcanti, I. F. A., Goswami, P., & Zhou, T. (2013). Monsoons in a changing world: A regional perspective in a global context. *Journal of Geophysical Research: Atmospheres*, 118(8), 3053–3065. <https://doi.org/10.1002/jgrd.50258>
- Lenssen, N. J. L., Schmidt, G. A., Hansen, J. E., Menne, M. J., Persin, A., Ruedy, R., & Zys, D. (2019). Improvements in the GISTEMP uncertainty model. *Journal of Geophysical Research: Atmospheres*, 124(12), 6307–6326. <https://doi.org/10.1029/2018JD029522>
- Li, G., Chen, L., & Lu, B. (2023). A physics-based empirical model for the seasonal prediction of the central China July precipitation. *Geophysical Research Letters*, 50(3), e2022GL101463. <https://doi.org/10.1029/2022GL101463>
- Li, G., & Xie, S.-P. (2014). Tropical biases in CMIP5 multi-model ensemble: The excessive equatorial Pacific cold tongue and double ITCZ problems. *Journal of Climate*, 27(4), 1765–1780. <https://doi.org/10.1175/JCLI-D-13-00337.1>
- Li, G., Xie, S.-P., Du, Y., & Luo, Y. (2016). Effects of excessive equatorial cold tongue bias on the projections of tropical Pacific climate change. Part I: The warming pattern in CMIP5 multi-model ensemble. *Climate Dynamics*, 47(12), 3817–3831. <https://doi.org/10.1007/s00382-016-3043-5>
- Li, G., Xie, S.-P., He, C., & Chen, Z. (2017). Western Pacific emergent constraint lowers projected increase in Indian summer monsoon rainfall. *Nature Climate Change*, 7(10), 708–712. <https://doi.org/10.1038/nclimate3387>
- Liu, X., & Yanai, M. (2001). Relationship between the Indian monsoon rainfall and the tropospheric temperature over the Eurasian continent. *Quarterly Journal of the Royal Meteorological Society*, 127(573), 909–937. <https://doi.org/10.1002/qj.49712757311>
- Luo, H., Wang, Z., He, C., Chen, D., & Yang, S. (2024). Future changes in South Asian summer monsoon circulation under global warming: Role of the Tibetan Plateau latent heating. *npj Climate and Atmospheric Science*, 7(1), 103. <https://doi.org/10.1038/s41612-024-00653-x>
- Lv, S., Song, F., Dong, H., & Wu, L. (2024). Phase and amplitude changes in rainfall annual cycle over global land monsoon regions under global warming. *Geophysical Research Letters*, 51(12), e2024GL108496. <https://doi.org/10.1029/2024GL108496>
- Misra, V., Bhardwaj, A., & Noska, R. (2017). Understanding the variations of the length and the seasonal rainfall anomalies of the Indian summer monsoon. *Journal of Climate*, 30(5), 1753–1763. <https://doi.org/10.1175/JCLI-D-16-0501.1>
- Moon, S., & Ha, K.-J. (2017). Temperature and precipitation in the context of the annual cycle over Asia: Model evaluation and future change. *Asia-Pacific Journal of Atmospheric Sciences*, 53(2), 229–242. <https://doi.org/10.1007/s13143-017-0024-5>
- Myhre, G., Samset, B. H., Hodnebrog, Ø., Andrews, T., Boucher, O., Faluvegi, G., et al. (2018). Sensible heat has significantly affected the global hydrological cycle over the historical period. *Nature Communications*, 9(1), 1922. <https://doi.org/10.1038/s41467-018-04307-4>
- Neelin, J. D., & Su, H. (2005). Moist teleconnection mechanisms for the tropical South American and Atlantic sector during El Niño. *Journal of Climate*, 18(8), 3928–3950. <https://doi.org/10.1175/JCLI3517.1>
- Pathirana, G., Shin, N. Y., Wu, Y. K., Kwon, M., & Kug, J. S. (2024). Intermodel relation between present-day warm pool intensity and future precipitation changes. *Climate Dynamics*, 62(1), 345–355. <https://doi.org/10.1007/s00382-023-06918-0>
- Previdi, M., Smith, K. L., & Polvani, L. M. (2021). Arctic amplification of climate change: A review of underlying mechanisms. *Environmental Research Letters*, 16(9), 093003. <https://doi.org/10.1088/1748-9326/ac1c29>
- Rajesh, P. V., & Goswami, B. N. (2022). A new emergent constraint corrected projections of Indian summer monsoon rainfall. *Geophysical Research Letters*, 49(8), e2021GL096671. <https://doi.org/10.1029/2021GL096671>
- Rajesh, P. V., Goswami, B. N., Choudhury, B. A., & Zahan, Y. (2021). Large sensitivity of simulated Indian summer monsoon rainfall (ISMR) to global warming: Implications of ISMR projections. *Journal of Geophysical Research: Atmospheres*, 126(1), e2020JD033511. <https://doi.org/10.1029/2020JD033511>
- Rayner, N. A. A., Parker, D. E., Horton, E. B., Folland, C. K., Alexander, L. V., Rowell, D. P., et al. (2003). Global analyses of sea surface temperature, sea ice, and night marine air temperature since the late nineteenth century. *Journal of Geophysical Research*, 108(D14). <https://doi.org/10.1029/2002JD002670>
- Rohde, R., Muller, R., Jacobsen, R., Perlmutter, S., & Mosher, S. (2013). Berkeley Earth temperature averaging process. *Geoinformatics & Geostatistics: An Overview*, 01(02), 1–7. <https://doi.org/10.4172/2327-4581.1000103>
- Sabeerali, C. T., & Ajayamohan, R. S. (2018). On the shortening of Indian summer monsoon season in a warming scenario. *Climate Dynamics*, 50(5–6), 1609–1624. <https://doi.org/10.1007/s00382-017-3709-7>
- Sabeerali, C. T., Rao, S. A., Ajayamohan, R. S., & Murtagudde, R. (2012). On the relationship between Indian summer monsoon withdrawal and Indo-Pacific SST anomalies before and after 1976/1977 climate shift. *Climate Dynamics*, 39(3), 841–859. <https://doi.org/10.1007/s00382-011-1269-9>
- Saha, P., Mahanta, R., & Goswami, B. N. (2023). Present and future of the South Asian summer monsoon's rainy season over Northeast India. *npj Climate and Atmospheric Science*, 6(1), 170. <https://doi.org/10.1038/s41612-023-00485-1>

- Sahana, A. S., Ghosh, S., Ganguly, A., & Murtugudde, R. (2015). Shift in Indian summer monsoon onset during 1976/1977. *Environmental Research Letters*, 10(5), 054006. <https://doi.org/10.1088/1748-9326/10/5/054006>
- Shamal, M., & Sanjay, J. (2021). An observational equatorial Atlantic Ocean constraint on Indian monsoon precipitation projections. *Climate Dynamics*, 57(1–2), 209–221. <https://doi.org/10.1007/s00382-021-05703-1>
- Smith, T. M., Reynolds, R. W., Peterson, T. C., & Lawrimore, J. (2008). Improvements to NOAA's historical merged land-ocean surface temperature analysis (1880–2006). *Journal of Climate*, 21(10), 2283–2296. <https://doi.org/10.1175/2007JCLI2100.1>
- Su, H., Neelin, J. D., & Meyerson, J. (2003). Sensitivity of tropical tropospheric temperature to sea surface temperature forcing. *Journal of Climate*, 16(9), 1283–1301. <https://doi.org/10.1175/1520-0442-16.9.1283>
- Subash, N., Dutta, D., Ghasal, P. C., Punia, P., Mandal, V. P., Chaudhary, V. P., & Prakash Chaudhary, V. (2023). Relevance of climatological information on spatial and temporal variability of Indian Summer monsoon rainfall (ISM) in recent El Niño years and its impact on four important kharif crops over India. *Climate Services*, 30, 100370. <https://doi.org/10.1016/j.cleser.2023.100370>
- Sun, M., Chen, L., Li, T., & Luo, J. J. (2023). CNN-based ENSO forecasts with a focus on SST zonal pattern and physical interpretation. *Geophysical Research Letters*, 50(20), e2023GL105175. <https://doi.org/10.1029/2023GL105175>
- Tokarska, K. B., Stolpe, M. B., Sippel, S., Fischer, E. M., Smith, C. J., Lehner, F., & Knutti, R. (2020). Past warming trend constrains future warming in CMIP6 models. *Science Advances*, 6(12), eaaz9549. <https://doi.org/10.1126/sciadv.aaz9549>
- Turner, A. G., & Annamalai, H. (2012). Climate change and the South Asian summer monsoon. *Nature Climate Change*, 2(8), 587–595. <https://doi.org/10.1038/nclimate1495>
- Vose, R. S., Arndt, D., Banzon, V. F., Easterling, D. R., Gleason, B., Huang, B., et al. (2012). NOAA's merged land-ocean surface temperature analysis. *Bulletin of the American Meteorological Society*, 93(11), 1677–1685. <https://doi.org/10.1175/BAMS-D-11-00241.1>
- Wang, L., Cheng, Y., Chen, X., & Zhou, T. (2024). Projected changes in onset of summer monsoon over the South Asian Marginal Seas Modulated by Intraprogressional Oscillation. *Journal of Climate*, 37(3), 821–835. <https://doi.org/10.1175/JCLI-D-23-0257.1>
- Webster, P. J., & Yang, S. (1992). Monsoon and ENSO: Selectively interactive systems. *Quarterly Journal of the Royal Meteorological Society*, 118(507), 877–926. <https://doi.org/10.1002/qj.49711850705>
- Wu, G., & Liu, B. (2014). Roles of forced and inertially unstable convection development in the onset process of Indian summer monsoon. *Science China Earth Sciences*, 57(7), 1438–1451. <https://doi.org/10.1007/s11430-014-4865-9>
- Xavier, P. K., Marzin, C., & Goswami, B. N. (2007). An objective definition of the Indian summer monsoon season and a new perspective on the ENSO–monsoon relationship. *Quarterly Journal of the Royal Meteorological Society*, 133(624), 749–764. <https://doi.org/10.1002/qj.45>
- Xie, S. P., Deser, C., Vecchi, G. A., Ma, J., Teng, H., & Wittenberg, A. (2010). Global warming pattern formation: Sea surface temperature and rainfall. *Journal of Climate*, 23(4), 966–986. <https://doi.org/10.1175/2009JCLI3329.1>
- Zhang, H., Liang, P., Moise, A., & Hanson, L. (2012). Diagnosing potential changes in Asian summer monsoon onset and duration in IPCC AR4 model simulations using moisture and wind indices. *Climate Dynamics*, 39(9–10), 2465–2486. <https://doi.org/10.1007/s00382-012-1289-0>
- Zhou, X., Wang, L., Hsu, P., Li, T., & Xiang, B. (2024). Understanding the factors controlling MJO prediction skill across events. *Journal of Climate*, 37(20), 5323–5336. <https://doi.org/10.1175/JCLI-D-23-0635.1>